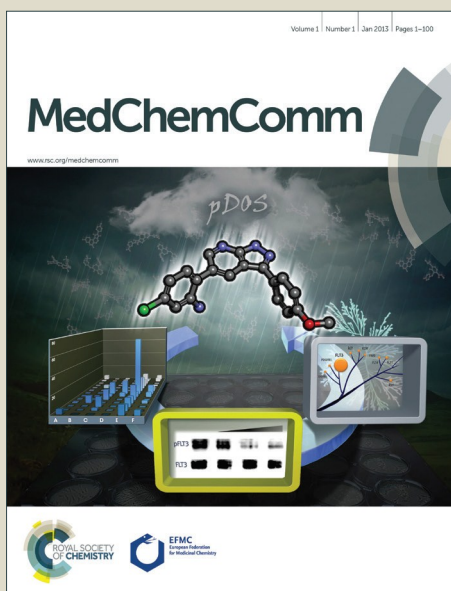


# MedChemComm

Accepted Manuscript



This is an *Accepted Manuscript*, which has been through the Royal Society of Chemistry peer review process and has been accepted for publication.

*Accepted Manuscripts* are published online shortly after acceptance, before technical editing, formatting and proof reading. Using this free service, authors can make their results available to the community, in citable form, before we publish the edited article. We will replace this *Accepted Manuscript* with the edited and formatted *Advance Article* as soon as it is available.

You can find more information about *Accepted Manuscripts* in the [Information for Authors](#).

Please note that technical editing may introduce minor changes to the text and/or graphics, which may alter content. The journal's standard [Terms & Conditions](#) and the [Ethical guidelines](#) still apply. In no event shall the Royal Society of Chemistry be held responsible for any errors or omissions in this *Accepted Manuscript* or any consequences arising from the use of any information it contains.



## Amyloid $\beta$ Derived Switch-Peptides as a Tool for Investigation of Early Events of Aggregation: A Combined Experimental and Theoretical Approach†

Received 00th January 20xx,  
Accepted 00th January 20xx

DOI: 10.1039/x0xx00000x

www.rsc.org/

Ashim Paul, Bhanita Sharma, Tanmay Mondal, Kishore Thalluri, Sandip Paul and Bhubaneswar Mandal\*

Alzheimer's disease, a severe neurodegenerative disorder, is believed to be caused by the interneuronal aggregation of Amyloid  $\beta$  peptide. It has no cure yet. Despite rigorous research, the mechanism of aggregation is also not fully delineated. Especially probing the early events of the aggregation is difficult as we have no control on the kinetics of the process of aggregation. We have used amyloid  $\beta$  derived switch-peptides that behaves as the functional mimic of Amyloid  $\beta$  peptide, and demonstrated that the side chain aromatic interaction precedes to the  $\beta$ -sheet formation resulting fibrillization. The detailed investigation on the early events of aggregation have become possible as the kinetics of aggregation of the switch-peptides can be controlled. We have used ultra-violet (UV), circular dichroism (CD), Raman spectroscopy and Molecular Dynamics (MD) Simulation as combined experimental and theoretical approach.

### Introduction

Alzheimer's disease, a devastating neurodegenerative disorder, is caused by the interneuronal aggregation of Amyloid- $\beta$  peptide (A $\beta$ , a 39 to 42 residue peptide) as amyloid plaque.<sup>1</sup> Since A $\beta$  peptide is highly amyloidogenic, its synthesis, purification, and monitoring fibrillogenesis by biophysical techniques are difficult, the mechanism of A $\beta$  aggregation, especially the early events, is still elusive.<sup>2,3</sup> But understanding the mechanism is important as it may lead to novel therapeutic approaches for perturbation of amyloidogenesis. Mutter's group have introduced the conformational switch-peptides by incorporation of an intramolecular O to N acyl migration based molecular switch that allows for the controlled initiation of folding process even in amyloid forming polypeptides.<sup>4,5</sup>

UV absorbance is a useful probe for constructing structure and structural changes of protein<sup>6</sup> as chromophores display shifted spectra upon changing polarity of their environment.<sup>7</sup> Proteins are known to absorb mostly at 240-310 nm due to the presence of the aromatic rings of Trp, Tyr and Phe. The amide group of peptide backbone absorbs strongly below 230 nm due to  $n \rightarrow \pi^*$  and  $\pi \rightarrow \pi^*$  electronic transitions, whereas aromatic residues absorb in the near-UV region between 250 and 290 nm due to  $\pi \rightarrow \pi^*$  electronic transitions.<sup>7b</sup> Since, the change in UV due to conformational transition is very small, circular dichroism (CD) is preferred.<sup>8</sup> The difference in the arrangement

of the chromophores gives rise to the difference in splitting of the electronic transitions:  $\pi \rightarrow \pi^*$  and  $n \rightarrow \pi^*$  transitions in  $\alpha$ -helix and  $\beta$ -sheet alters the absorption spectra and the CD spectra of polypeptides.<sup>8a</sup> In addition to splitting of electronic transitions, the placement of chromophores in ordered arrays leads to hypo or hyperchromism of their optical transitions and it was evident that the  $\alpha$ -helical peptide is hypochromic while the peptide in  $\beta$ -sheet conformation is hyperchromic.<sup>9</sup> Similarly,  $\alpha$ -helix to  $\beta$ -sheet transitions causes a change in vibrational modes of various bonds in a peptide and the change is widely characterized by Raman Spectroscopy.<sup>10</sup> In aqueous solution, the amide I band of the peptide are obscured by the bending vibration modes of H<sub>2</sub>O in Infra-red (IR) spectroscopy but such interference is lesser in Raman spectroscopy.<sup>11</sup> Therefore, in aqueous medium the conformational change may also be monitored by Raman spectroscopy.

However, the initializations of association of proteins are difficult to characterize in molecular details by experimental methods due to the dynamic equilibrium between dimers, trimers, tetramers, *etc.*, of the self-assembled proteins. Therefore, molecular dynamics simulation of protein aggregation can complement the experimental results in the study of amyloid aggregation and can provide insights into the early steps of protein aggregation.

Herein, we have demonstrated that the early events of aggregation of amyloidogenic peptides can be investigated in microscopic detail using specially designed switch-peptides that allows for the retardation of the kinetics of aggregation. A parallel UV, CD and Raman spectroscopic analyses as well as MD simulations have been carried out.

Department of Chemistry, Indian Institute of Technology Guwahati, Assam-781039, India. Email: bmandal@iitg.ernet.in

† Electronic Supplementary Information (ESI) available: See DOI: 10.1039/x0xx00000x

## Results and discussion

To prove our hypothesis, we synthesized two switch-peptides,<sup>4a</sup> AcSLSL-(H<sup>+</sup>)S-LSLSLGNH<sub>2</sub> (**1**), AcSLSLHQKL VFF-(H<sup>+</sup>)S-EDVSLGNH<sub>2</sub> (**2**) and two  $\beta$ -sheet breaker peptides,<sup>12</sup> AcLPPFDNH<sub>2</sub> (**3**), AcLVFFDNH<sub>2</sub> (**4**). The switch-peptide **1** does not contain any aromatic ring in the side chain (for simplification of analysis) but **2** contain two phenyl rings in the side chain.<sup>4</sup> The peptides were characterized by HPLC and mass spectrometry (Fig. S1-S8, ESI). Both of these switch-peptides converted their conformation from random coil (rc) to  $\beta$ -sheet upon pH triggering (*i.e.* O to N acyl migration,  $t_{1/2} \approx 23.2$  min for peptide **2** in PBS of pH 7.4 at 37 °C, Fig. S9, ESI), which finally resulted in amyloid formation.<sup>4a</sup> The peptides formed clear fibrillar structure when viewed under TEM and also showed characteristic green gold birefringence under cross polarized light when stained with Congo red dye (Fig. S10, ESI).<sup>13</sup> The kinetics of amyloid formation was monitored by a time dependent Thioflavin T fluorescence assay (Fig. S11, ESI).

Since, the switch-peptides form amyloid fibril<sup>4</sup> as A $\beta$  peptide does, we went for further investigations on the early events of amyloid formation using them. The UV and CD spectra of **1** recorded at the initial time ( $t = 0$ , Fig. 1) and after completion of the conformational transition ( $t = 50$  min, Fig. 1) is depicted. There was a small but consistent change in the UV absorption spectra of **1** recorded at  $t = 0$  and  $t = 50$  min (Fig. 1a) of triggering the switch. This is essentially due to the conformational change of the peptide as no other change in the experimental conditions was allowed. During the time of observation, the peptide was converted from rc to  $\beta$ -sheet conformation that was verified by parallel CD analysis (Fig. 1b). The CD curve at  $t = 0$  was characteristic of a rc, whereas that at 50 min was characteristic of a  $\beta$ -sheet conformation. Moreover, UV spectra obtained from poly-L-lysine<sup>7b</sup> due to rc to  $\beta$ -sheet transition by Rosenheck and Doty resembles to our results (Fig. 1a). The  $\pi \rightarrow \pi^*$  (centred at 200 nm)<sup>9,14</sup> transition was influenced significantly by rc to  $\beta$ -sheet transition of **1** due to the decrease in polarity of the environment of the amide bond.<sup>7a</sup> However, the change in absorbance at 220 nm, which arises due to  $n \rightarrow \pi^*$  transitions was also notable.

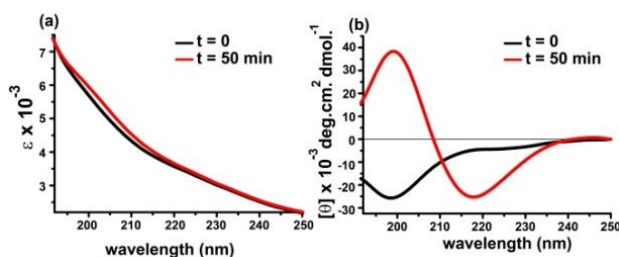


**Fig. 1.** Change in (a) UV spectra and (b) CD spectra, due to conformational transition of **1** ( $c = 50 \mu\text{M}$ , PBS pH 7.4 at 37 °C) occurred in 50 min.

A comparison of the regular changes in the UV absorbance and the ellipticity at 220 nm due to a rc to  $\beta$ -sheet transition of **1** was monitored in a time dependent manner (Fig. 2). The half life ( $t_{1/2}$ ) of  $\beta$ -sheet elongation was obtained by fitting the

experimental curve with Boltzmann equation. The  $t_{1/2}$  value ( $13.95 \pm 0.6$  min) obtained in this manner was in accordance with that obtained by CD measurement ( $12.76 \pm 0.3$  min).

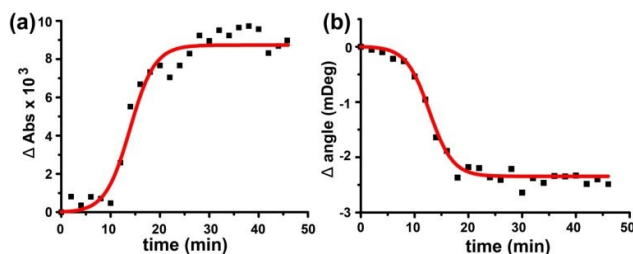


**Fig. 2.** Time course measurement of the rc  $\rightarrow$   $\beta$ -sheet transition of **1**, monitored by (a) UV absorbance (sigmoid fit,  $R^2 = 0.98$ ) and (b) CD (sigmoid fit,  $R^2 = 0.99$ ) ( $c = 20 \mu\text{M}$ , PBS pH 7.4, at 220 nm).

Similar change in the UV and CD spectra upon conformational (rc to  $\beta$ -sheet) transition was noticed for all other switch-peptides tested and the switch peptide-inhibitor mixtures. Therefore, the change in the UV and CD absorption was accepted as a characteristic feature of the conformational change of the switch-peptides. Switch-peptide **2** used in this work neither contain Trp nor Tyr but Phe. Phe has a smaller extinction coefficient compared to Trp or Tyr because of its high symmetry.<sup>7a</sup> However, evolution of two positive bands at 265 and 285 nm in the near UV range of the CD due to aggregation is reported for amylin peptide.<sup>15</sup> It is believed that, these two positive bands centred at 265 and 285 nm are due to the conformational restrictions of the aromatic rings of Phe15, Phe23 and Tyr37, associated with aromatic interactions that may be related to  $\beta$ -sheet stacking. As the rc to  $\beta$ -sheet transition associated with the aggregation of the amylin peptide influenced its near UV CD spectra due to the  $\pi \rightarrow \pi^*$  electronic transition of the aromatic side chains, it is expected to influence similarly the near UV absorption spectra also. A time course measurement of UV absorption at 220 and 257 nm of **2** was compared with the evolution of CD signals at 220 nm (Fig. 3). The aim here was to study the effect of the onset of  $\beta$ -sheet structure on the environmental alteration of the aromatic side chain of Phe. As discussed before, the absorption and the ellipticity at 220 nm indicate particularly the onset of  $\beta$ -sheets. On the other hand, the absorbance due to the amide chromophore is negligible compared to  $\pi \rightarrow \pi^*$  transition of aromatic side chains at near UV region. Therefore, the chronological change of the absorbance at 257 nm is expected to be influenced exclusively by the environmental alteration of the aromatic side chain of Phe residues resulting from conformational transitions. Therefore, although the extinction coefficient of Phe is higher at 206 nm and 188 nm than at 257 nm, absorbance at 257 nm was preferred to investigate the environmental change of Phe.

As in case of **1**, the time of half conversion of rc to  $\beta$ -sheet at 20  $\mu\text{M}$  of **2** ( $t_{1/2} = 37.1 \pm 0.4$  min), revealed by monitoring the change in absorbance at 220 nm (black, Fig. 3a), corresponded well with the  $t_{1/2}$  obtained by monitoring the ellipticity ( $t_{1/2} = 41.4 \pm 0.6$  min) at 220 nm (black, Fig. 3d). The results again support the inference that kinetics of rc to  $\beta$ -sheet

transition of the switch-peptides can be measured by monitoring the UV absorption at 220 nm. Moreover,  $t_{1/2}$  determined by measuring the change in absorbance at 257 nm also followed similar order ( $t_{1/2} = 31.5 \pm 0.4$  min). This implies a regular environmental change of the aromatic side chain of Phe occurred in parallel to the rc to  $\beta$ -sheet transition. However, the ellipticity values at 257 nm were unchanged (red, Fig. 3d) as no cotton effect is expected at that wavelength. The increase in UV absorbance at 257 nm due to the conformational transition was associated with the aromatic interactions related to  $\beta$ -sheet stacking<sup>15</sup> and through-space intermolecular interactions among the newly formed  $\beta$ -sheets.<sup>16</sup> Therefore, this increase in absorbance may directly be related to the nucleation phenomenon initiated by aromatic stacking of Phe.

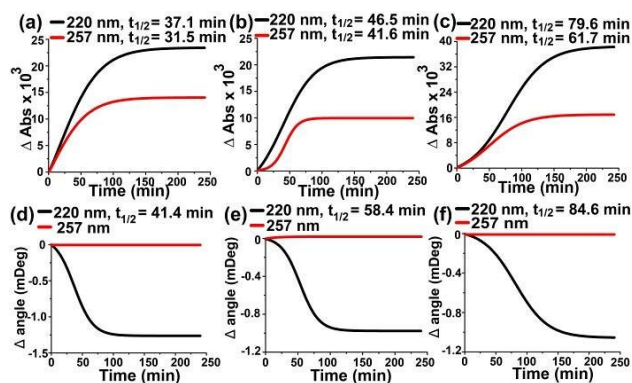


**Fig. 3.** Normalized sigmoid fit of the change in absorbance (a, b and c) and ellipticity (d, e and f) at 220 nm and 257 nm of **2**. (c = 20  $\mu$ M (a, d), 10  $\mu$ M (b, e) and 5  $\mu$ M (c, f) in PBS, pH 7.4, 37°C).

Varying the concentration of **2** exerted similar effects on the time course of the change in UV absorption at 257 nm (10  $\mu$ M, Fig. 3b and 5  $\mu$ M, Fig. 3c) and the change in ellipticity at 220 nm (10  $\mu$ M, Fig. 3e and 5  $\mu$ M, Fig. 3f). The increment of  $t_{1/2}$ , due to aromatic stacking, from  $31.5 \pm 0.4$  min (at 20  $\mu$ M) to  $41.6 \pm 0.5$  min (at 10  $\mu$ M) and further increment to  $61.7 \pm 0.9$  min (at 5  $\mu$ M) as obtained by monitoring the UV absorption at 257 nm corresponded well with the  $t_{1/2}$  of the onset of  $\beta$ -sheet formation as obtained by the change in ellipticity at 220 nm from  $41.4 \pm 0.6$  min (at 20  $\mu$ M) to  $58.4 \pm 0.7$  min (at 10  $\mu$ M) and further to  $84.6 \pm 1.0$  min (at 5  $\mu$ M). Slower transitions at lower concentration are reasonable as decreasing concentration usually delays nucleation.

Interestingly, at each concentrations (20, 10 and 5  $\mu$ M) tested; the  $t_{1/2}$  of aromatic stacking was smaller than the corresponding  $t_{1/2}$  of onset of  $\beta$ -sheet formation (backbone H-bonding interactions). These results imply that the aromatic stacking takes place prior to  $\beta$ -sheet formation in the process of aggregation. That implies, aromatic stacking occurs at an earlier stage of  $\beta$ -sheet formation. Nevertheless, these results suggest that one can follow the early onset of  $\beta$ -sheet formation of **2** in microscopic detail by combined UV and CD measurements.

The changes in amide I vibration due to rc to  $\beta$ -sheet transformation was monitored by Raman spectroscopy also. At  $t = 0$ , the amide I band at  $1665 \text{ cm}^{-1}$  that corresponds to rc or  $\alpha$ -helical conformation (Fig. S12a, ESI) was suppressed significantly with time and a new band at  $1633 \text{ cm}^{-1}$  was observed that corresponds to  $\beta$ -sheet conformation (at 90 min).

The presence of Phe in **2** also exhibited a characteristic band at  $\sim 1020 \text{ cm}^{-1}$  (Fig. S12b, ESI). There was no shift of the band during rc to  $\beta$ -sheet conversion but increment of the intensity with time was observed.<sup>10,17</sup>

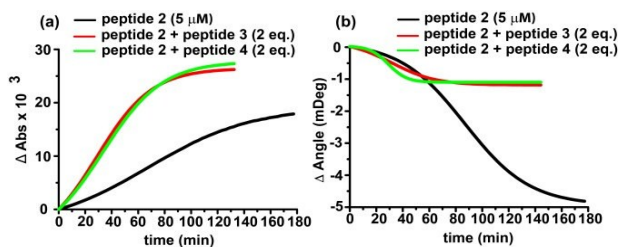


**Fig. 4.** Effect of the inhibitors on (a) the aromatic stacking monitored by change in absorbance at 257 nm and (b) the onset of  $\beta$ -sheet formation monitored by change in ellipticity at 220 nm of **2** (5  $\mu$ M) in PBS of pH 7.4 at 37°C

To confirm our hypothesis that the aromatic stacking precedes  $\beta$ -sheet formation and fibrillogenesis further, a comparative UV and CD studies were performed in presence of inhibitors. Well known  $\beta$ -sheet breaker peptides **3** and **4** were selected as inhibitors.<sup>8</sup> The effect of mixing two equivalents of **3** and **4** on the onset of  $\beta$ -sheet formation of **2** (5  $\mu$ M) is shown in Fig. 4 (red and green curve respectively). Fig. 4a shows the change in absorbance at 257 nm, while Fig. 4b shows the onset of  $\beta$ -sheet formation as observed by monitoring the change in ellipticity at 220 nm. At 5  $\mu$ M of **2**, mixing with the inhibitors resulted in higher absorbance (red and green, Fig. 4a) than the absorbance noted in the absence of the inhibitor (black, Fig. 4a). This elevation of absorbance resembles to the situation where the concentration of **2** was increased (Fig. 3) although the concentration of **2** was unaltered; instead, two equivalents of Phe containing inhibitor were added. Therefore, it is inferred that this increment in absorbance resulted from the interaction between the inhibitor and the switch-peptide due to aromatic stacking. Interestingly, parallel CD studies (at 220 nm) exhibited a decrease of  $\beta$ -sheet formation in the presence of the inhibitors (Fig. 4b) indicating a significant inhibition of  $\beta$ -sheet formation. Thus, the recognition of the inhibitors by the switch-peptide occurred due to the intermolecular aromatic interaction, which finally resulted in an inhibition of  $\beta$ -sheet formation.

To understand the initial stages of aggregation of our switch-peptides in molecular details, we have carried out classical molecular dynamics (MD) simulation of five molecules of switch-peptide (**2**,  $S_{on}$  state) in 10,000 water molecules. We have prepared three different systems, of which, in system S0, the peptides were randomly placed in the simulation box in the initial structure. As it is expected that the potential to form fibril structure originate in the sequence of peptide, in system S1, we have arranged the five switch-peptides parallel to each other with a distance of 7 Å apart to see the fibril formation and its stabilization in water. The presence of  $\beta$ -breaker peptides may influence the fibril formation by disturbing the hydrophobic, hydrophilic or stacking interactions. From our experimental study discussed above it is observed that the inhibition of aromatic interaction between switch-peptides results in an inhibition of  $\beta$ -sheet



formation. So in system S2, we placed ten molecules of  $\beta$ -breaker peptides, five of sequence **3**, and five of sequence **4**, in between the parallel arrangement of switch-peptides as the initial structure. An overview of all the systems is briefly summarized in Table 1.

Systems	No. of Peptide <b>2</b>	Initial arrangement of <b>2</b>	No. of $\beta$ -Breakers	No. of Water	Box Volume (nm <sup>3</sup> )
S0	5	Random	0	10,000	313.60
S1	5	Parallel	0	10,000	313.05
S2	5	Parallel	10	10,000	322.69

**Table 1** Overview of systems.

Due to long chain length with 18 amino acids in the switch-peptide **2**, formation of ordered  $\beta$ -sheet structures is least expected in MD simulation, as our simulations are carried out without any constrain. Still, the early stages of peptide aggregation can well be understood from our simulations. The snap-shots taken at different time intervals for system S0 (Fig. 5a) support our prediction that the aromatic stacking (due to Phe-Phe interactions) occurs prior to fibril formation. In specific, the Phe-Phe interactions are responsible for the formation of dimers first and then to oligomers. In Fig. 5b, snap-shots at different time-steps for systems S1 with contour density plots of Phe residues show that the fibril formation is mostly stabilized by Phe-Phe interactions. The presence of  $\beta$ -breakers in systems S2 significantly reduces the formation of amyloid fibrils due to intermolecular aromatic interaction between Phe residue of switch-peptides and the  $\beta$ -breakers, and the snap-shots are shown in Fig. 5c. To understand the effect of Phe-Phe interactions on peptide aggregation, we have calculated the radial distribution functions (rdf),  $g(r)$ , between intermolecular Phe residues of **2** and these are shown in Fig. 6. The peak heights indicate the probability of finding a Phe near a reference Phe.

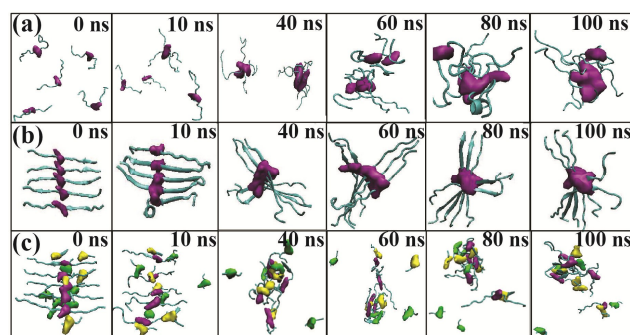


**Fig. 5.** Snap-shots of protein-protein association at different time steps when peptides were (a) placed randomly in the simulation box, (b) arranged parallel to each other at a distance of 7 Å, (c) arranged parallel to each other at a distance of 7 Å, and  $\beta$ -breaker peptides are placed in between the protein. Contour density of Phe residues are shown in purple colour (a, b and c) and that of  $\beta$ -breakers are shown in yellow and green colour (c).

The height of the first peak observed maximum for system S1 where all the peptides were arranged parallel to each other in the initial structure. The formation of higher order peaks can be seen due to the interactions of Phe residues in the parallel

arrangement of peptides. System S0 doesn't show any clear higher order peaks as the peptides were randomly placed in the simulation box. In presence of  $\beta$ -breaker (for system S2), we see a shifting in position of the first peak and depletion in the peak heights. This is due to the fact of interaction between Phe groups of  $\beta$ -breaker and the switch-peptides, which reduces the Phe-Phe intermolecular interactions between the switch-peptides. In Figure 6 (b), we have shown Phe-Phe rdfs involving switch-peptide and  $\beta$ -breaker for system S2. It can be seen that the interaction of Phe residues of  $\beta$ -breaker with peptides is much stronger than the Phe-Phe interactions of switch-peptides.

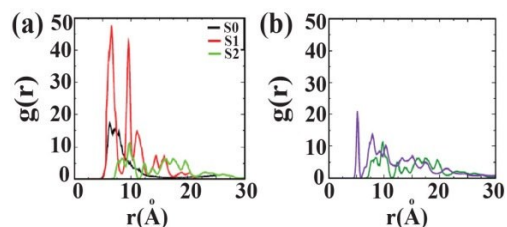


**Fig. 6.** Radial distribution functions of (i) Phe-Phe for **2** of systems S0, S1, S2, (ii) Phe-Phe rdf between switch-peptides (black), and between  $\beta$ -breaker and switch-peptides (red) for system S2.

The hydration number around Phe groups can further provide us the information about the interaction of water molecules with Phe groups, which in turn can throw some lights on Phe-Phe interactions. Therefore, in Table 2, we have shown the number of first shell water molecules around Phe residue of peptides. The first shell coordination number is defined as:

$$n_{\alpha\beta} = 4\pi\rho_{\beta} \int_0^{r_c} r^2 g_{\alpha\beta}(r) dr$$

Where,  $n_{\alpha\beta}$  corresponds to the number of atom type  $\beta$  surrounding atom type  $\alpha$  in a shell extending from 0 to  $r_c$ .  $\rho_{\beta}$  and  $r_c$  are the number density of  $\beta$  in the system and the position of the first minimum in the corresponding radial distribution function (rdf).

System	Hydration Number	HBprotein-protein	HBprotein-water
S0	2.95	9.36	70.34
S1	2.36	13.54	53.90
S2	2.51	6.11	66.04

**Table 2.** The hydration number around residue Phe of **2** and the number of protein-protein (per protein) and protein-water (per protein) hydrogen bonds in different systems. The estimated standard deviation for all data is less than 0.002.

In presence of  $\beta$ -breaker, hydration number increases from 2.36 in system S1 to 2.51 in system S2, which depicts that more water is available around Phe residues of switch-peptides resulting from the breaking of parallel arrangement of proteins in S1. Interestingly, hydration number around Phe residues for S2 is lower than S0, though Phe-Phe rdfs show lowest peak for S2. This is because of the interaction of Phe residues of  $\beta$ -

breakers with Phe residues of switch-peptides, which restricts the interaction of water with switch-peptides, though peptide aggregation is the lowest in system S2. The inter-molecular  $\beta$ -sheet structures are stabilized predominantly by backbone hydrogen bonds and hydrophobic interactions.<sup>18</sup> A network of inter molecular H-bonds stabilizes the  $\beta$ -sheet structure once formed.<sup>19</sup> Therefore, we have also calculated average number of protein-protein and protein-water H-bonds per switch-peptide and they are listed in the Table 2. The geometric criteria for calculating H-bonds are as follows: (i) the donor (D) and acceptor (A) distance is less than or equal to 3.4 Å and simultaneously (ii) the angle H-D-A is less than or equal to 45 °C. The number of protein-protein H-bonds per protein is the lowest for system S2, whereas number of protein-water H-bonds per protein is the highest for system S0. All these results are in similar trends with our rdf analysis and support our hypothesis.

The hypothesis that the aromatic stacking occurs prior to  $\beta$ -sheet formation was further supported by a reported molecular dynamic simulation study, which revealed that Phe-Phe pair prefers a stacked orientation (ideal for fibrillization) over a T-shaped configuration.<sup>20</sup> Our results also explain the findings of Gazit and colleagues that when Phe was replaced by Ala of the basic amyloidogenic unit of hIAPP (a peptide hormone, causes diabetes type II),<sup>15</sup> NFGAIL, the amyloidogenic potential of the pentapeptide was completely abolished.<sup>21</sup> On the other hand, when Phe was replaced by Trp, fibrillization became faster.<sup>22</sup>

Almost all known amyloid related aggregating proteins contain amino acids with aromatic side chains and the central role of stacking interactions in the self-assembly processes<sup>23</sup> are well accepted in chemistry and biochemistry, but such clear evidence of the same was not reported before. Furthermore, the results discussed herein are highly relevant in the wider context of aromatic or  $\beta$ -sheet stacking driven supra molecular self-assembly, which sometimes may help in designing novel material having important physical properties. For example, reversible self-assembly of oligo(p-phenylenevinylene) peptide conjugates in water is reported recently resulting in a stable fluorescent hydrogel upon pH changes.<sup>24</sup>

## Conclusions

Using a properly designed switch-peptide, detailed observation of the kinetics of the aromatic stacking and the  $\beta$ -sheet formation as two discrete processes that lead to fibrillization was possible for the first time. The experimental evidences suggest that aromatic interaction precedes conformational conversion, and also recognition of the aggregating switch-peptide and the inhibitor takes place prior inhibition. Also, the molecular level understanding of early stages of aggregation from our MD simulation study directly predicts the aromatic stacking as predominant interaction of peptide aggregation. These findings on the early events of aggregation are of utmost relevance for further studies on deciphering the mechanism of aggregation and finding out novel therapeutic strategies for combating protein conformational disorders. Also it may help in designing novel materials with interesting properties.

## Acknowledgements

We are thankful to DBT, India for financial support (BT/347/NE/TBP/2012); CIF, IIT Guwahati for LC-MS and TEM studies, also Prof. M. Mutter for important discussion.

## Notes and references

- (a) J. Hardy and D. J. Selkoe, *Science*, 2002, **297**, 353–356; (b) M. M. Luehmann, T. L. Spires-Jones, C. Prada, M. G. Alloza, A. D. Calignon, A. Rozkalne, J. K. Talboo, D. M. Holtzman, B. J. Bacskai and B. T. Hyman, *Nature*, 2008, **451**, 720–724.
- (a) M. M. Luehmann, J. Coomaraswamy, T. Bolmont, S. Kaeser, C. Schaefer, E. Kilger, A. Neuenschwander, D. Abramowski, P. Frey, A. L. Jatton, J. M. Vigouret, P. Paganetti, D. M. Walsh, P. M. Mathews, J. Ghiso, M. Staufenbiel, L. C. Walker and M. Jucker, *Science*, 2006, **313**, 1781–1784; (b) P. T. Lansbury Jr. and H. A. Lashuel, *Nature*, 2006, **443**, 774–779.
- (a) G. Liu, J. C. Gaines, K. J. Robbins and N. D. Lazo, *J. Am. Chem. Soc.*, 2010, **132**, 18223–18232; (b) D. M. Walsh, D. M. Hartley, Y. Kusumoto, Y. Fezoui, M. M. Condron, A. Lomakin, G. B. Benedek, D. J. Selkoe and D. B. Teplow, *J. Biol. Chem.*, 1999, **274**, 25945–25952; (c) I. Kheterpal, H. A. Lashuel, D. M. Hartley, T. Walz, P. T. Lansbury Jr. and R. Wetzel, *Biochemistry*, 2003, **42**, 14092–14098.
- (a) M. Mutter, A. Chandravarkar, C. Boyat, J. Lopez, S. D. Santos, B. Mandal, R. Mimna, K. Murat, L. Patiny, L. Saucedo and G. Tuchscherer, *Angew. Chem. Int. Ed.*, 2004, **43**, 4172–4178; (b) S. D. Santos, A. Chandravarkar, B. Mandal, R. Mimna, K. Murat, L. Saucedo, P. Tella, G. Tuchscherer and M. Mutter, *J. Am. Chem. Soc.*, 2005, **127**, 11888–11889; (c) M. S. Camus, S. D. Santos, A. Chandravarkar, B. Mandal, A. W. Schmid, G. Tuchscherer, M. Mutter and H. A. Lashuel, *ChemBioChem*, 2008, **9**, 2104–2112; (d) L. Saucedo, S. D. Santos, A. Chandravarkar, B. Mandal, R. Mimna, K. Murat, M. S. Camus, J. Berard, E. Grouzmann, M. Adrian, J. Dubochet, J. Lopez, H. Lashuel, G. Tuchscherer and M. Mutter, *Chimia*, 2006, **60**, 199–202.
- (a) L. Saucedo, S. D. Santos, A. Chandravarkar B. Mandal, R. Mimna, K. Murat, M. S. Camus, J. Berard, E. Grouzmann, M. Adrian, J. Dubochet, J. Lopez, H. A. Lashuel, G. Tuchscherer and M. Mutter, *Chimia*, 2006, **60**, 199–202; (b) R. Mimna, M. S. Camus, A. Schmid, G. Tuchscherer, H. A. Lashuel and M. Mutter, *Angew. Chem. Int. Ed.*, 2007, **46**, 2681–2684.
- M. E. Brewster, M. S. Hora, J. W. Simpkins, N. Bodor, *Pharm. Res.*, 1991, **8**, 792–795.
- (a) W. Colon, *Methods Enzymol.*, 1999, **309**, 605–632; (b) K. Rosenheck and P. Doty, *Proc. Natl. Acad. Sci. USA.*, 1961, **47**, 1775–1785.
- (a) N. Greenfield and G. D. Fasman, *Biopolymers*, 1969, **7**, 595–610; (b) N. A. Besley and J. D. Hirst, *J. Am. Chem. Soc.*, 1999, **121**, 9636–9644.

- 9 K. Rosenheck and B. Sommer, *J. Chem. Phys.*, 1967, **46**, 532–536.
- 10 (a) A. Rygula, K. Majzner, K. M. Marzec, A. Kaczor, M. Pilarczyk and M. Baranska, *J. Raman Spectrosc.*, 2013, **44**, 1061–1076; (b) S. A. Oladepo, K. Xiong and Z. Hong, *Chem. Rev.*, 2012, **112**, 2604–2628.
- 11 N. C. Maiti, M. M. Apetri, M. G. Zagorski, P. R. Carey and V. E. Anderson, *J. Am. Chem. Soc.*, 2004, **126**, 2399–2408.
- 12 (a) L. O. Tjernberg, J. Naslund, F. Lindqvist, J. Johansson, A. R. Karlstromi, J. Thyberg, L. Terenius and C. Nordstedt, *J. Biol. Chem.*, 1996, **271**, 8545–8548; (b) C. Soto, E. M. Sigurdsson, L. Morelli, R. A. Kumar, E. M. Castano and B. Frangione, *Nat. Med.*, 1998, **4**, 822–826.
- 13 (a) A. Paul, K. C. Nadimpally, T. Mondal, K. Thalluri and B. Mandal, *Chem. Commun.*, 2015, 51, 2245–2248; (b) K. C. Nadimpally, A. Paul and B. Mandal, *ACS Chem. Neurosci.*, 2014, **5**, 400–408.
- 14 R. W. Woody, *Theory of Circular Dichroism of Proteins*. Plenum Press, Newyork, 1996, 25–67.
- 15 R. Kayed, J. Bernhagen, N. Greenfield, K. Sweimeh, H. Brunner, W. Voelter and A. Kapurniotu, *J. Mol. Biol.*, 1999, **287**, 781–796.
- 16 R. W. Woody and K. Dumker, *Aromatic and cystine side-chain circular dichroism in proteins*. Plenum Press, New York and London, 1997, 109–158.
- 17 A. Bertoluzza, C. Fagnano, C. Caramazza, E. Barbaresi and S. Mancini, *J. Mol. Struct.*, 1989, **214**, 111–117.
- 18 R. Tycko, *Methods Enzymol.*, 2006, **413**, 103–122.
- 19 A. T. Petkova, W. M. Yau and R. Tycko, *Biochemistry*, 2006, **45**, 498–512.
- 20 R. Chelli, F. L. Garvasio, P. Procacci and V. Schettino, *J. Am. Chem. Soc.*, 2002, **124**, 6133–6143.
- 21 R. Azriel and E. Gazit, *J. Biol. Chem.*, 2001, **276**, 34156–34161.
- 22 Y. Porat, A. Stepensky, F. X. Ding, F. Naider and E. Gazit, *Biopolymers*, 2003, **69**, 161–164.
- 23 E. Gazit, *FASEB J.*, 2002, **16**, 77–83.
- 24 M. Mba, A. Moretto, L. Armelao, M. Crisma, C. Toniolo and M. Maggini, *Chem. Eur. J.*, 2011, **17**, 2044–2047.

## Graphical Abstract

**Title: Amyloid  $\beta$  Derived Switch-Peptides as a Tool for Investigation of Early Events of Aggregation: A Combined Experimental and Theoretical Approach****Authors: Ashim Paul, Bhanita Sharma, Tanmay Mondal, Kishore Thalluri, Sandip Paul and Bhubaneswar Mandal\***

The  $\pi \rightarrow \pi$  stacking interaction takes place prior to aggregation as the early event of amyloid aggregation of an amyloidogenic peptide.

